

# Symmetry Breaking in an Extended $O(2)$ Model

(arXiv:2312.17739)

Leon Hostetler <sup>1</sup>, Ryo Sakai <sup>2</sup>, Jin Zhang <sup>3</sup>, Alexei Bazavov <sup>1</sup>,  
and Yannick Meurice <sup>4</sup>

<sup>1</sup> Michigan State University

<sup>2</sup>Jij Inc.

<sup>3</sup>Chongqing University

<sup>4</sup>The University of Iowa

January 9, 2024

QuLAT Collaboration

# Outline

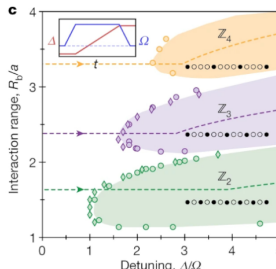
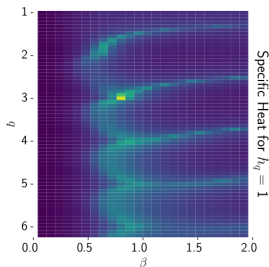
- 1 Motivation
- 2 The Extended-O(2) Model
  - The  $h_q \rightarrow \infty$  limit
  - Phase Diagram
- 3 Phase Diagram at Finite- $h_q$
- 4 Summary & Outlook

# Outline

- 1 Motivation
- 2 The Extended- $O(2)$  Model
  - The  $h_q \rightarrow \infty$  limit
  - Phase Diagram
- 3 Phase Diagram at Finite- $h_q$
- 4 Summary & Outlook

# Motivation

- 1 The  $O(2)$  model is a non-trivial limit of the Abelian-Higgs model
- 2 Can add a symmetry-breaking term to break the  $O(2)$  symmetry down to  $\mathbb{Z}_q$ 
  - ▶ Study the role of symmetry in spin systems
  - ▶ Study  $\mathbb{Z}_q$  approximations of continuous  $U(1)/O(2)$  symmetry
  - ▶ Relevant for “field digitization” of gauge theories
- 3 Playground for tensor methods
- 4 Early results suggested a phase diagram similar to that found in Rydberg atom chains (Bernien et. al. Nature 551, 579-584 (2017), Keesling et. al. Nature 568, 207 (2019))





# Outline

- 1 Motivation
- 2 The Extended-O(2) Model
  - The  $h_q \rightarrow \infty$  limit
  - Phase Diagram
- 3 Phase Diagram at Finite- $h_q$
- 4 Summary & Outlook

# The Extended-O(2) Model

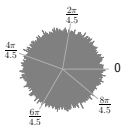
- We consider an extended-O(2) model in 2D with action

$$S_{\text{ext-O}(2)} = - \sum_{x, \mu} \cos(\varphi_{x+\hat{\mu}} - \varphi_x) - h_q \sum_x \cos(q\varphi_x)$$

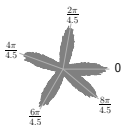
- When  $h_q = 0$ , this is the classic XY model, with a BKT transition
- When  $h_q \rightarrow \infty$ , the continuous angle  $\varphi$  is forced into the discrete values

$$\varphi_0 \leq \varphi_{x,k} = \frac{2\pi k}{q} < \varphi_0 + 2\pi$$

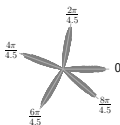
- For  $q \in \mathbb{Z}$ , this is the ordinary  $q$ -state clock model with  $\mathbb{Z}_q$  symmetry
- For  $q \notin \mathbb{Z}$ , this defines an interpolation of the clock model for noninteger  $q$



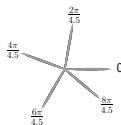
(a)  $h_q = 0$



(b)  $h_q = 1$



(c)  $h_q = 4$



(d)  $h_q = 64$

# The $h_q \rightarrow \infty$ limit

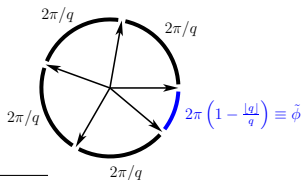
- In the limit  $h_q \rightarrow \infty$ , we can replace the action with

$$S_{\text{ext-}q} = - \sum_{x,\mu} \cos(\varphi_{x+\hat{\mu}} - \varphi_x)$$

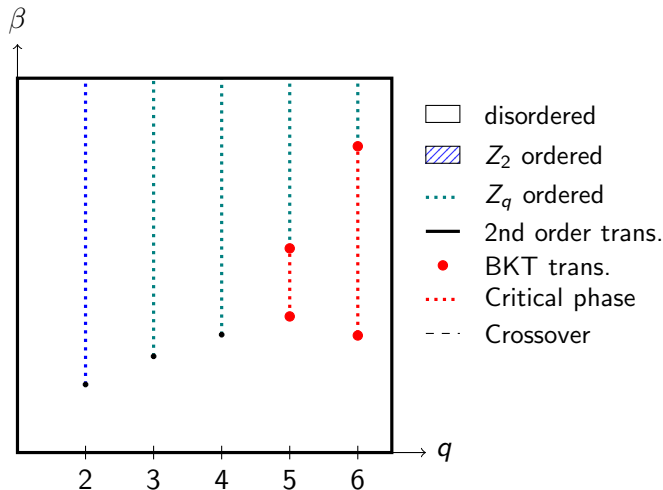
- We directly restrict the previously continuous angles to the discrete values

$$\varphi_0 \leq \varphi_{x,k} = \frac{2\pi k}{q} < \varphi_0 + 2\pi$$

- We choose  $\varphi_0 = 0$ , i.e.  $\varphi \in [0, 2\pi)$ , but we also investigate  $\varphi_0 = -\pi$
- For  $q \notin \mathbb{Z}$ , divergence from ordinary clock model behavior is driven by the introduction of a “small angle”:



# The $h_q \rightarrow \infty$ limit



# TRG results at large volume

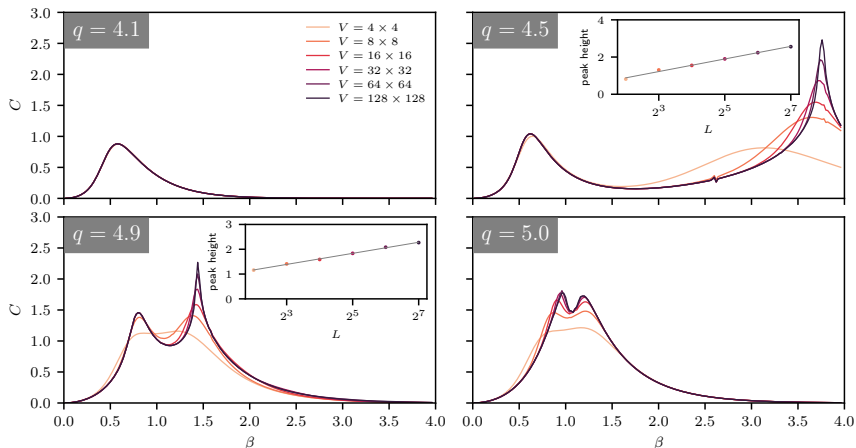
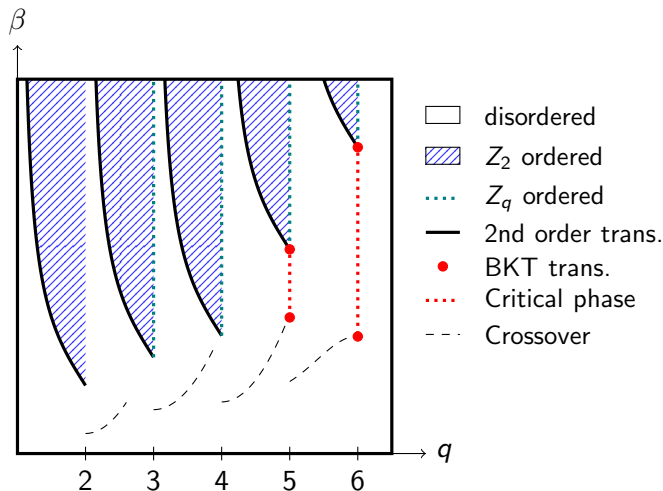


**Figure:** Specific heat results for the extended- $q$  clock model from TRG obtained by Ryo for  $q = 4.1, 4.5, 4.9$ , and  $5.0$  at volumes from  $2^2 \times 2^2$  up to  $2^7 \times 2^7$ .

# The $h_q \rightarrow \infty$ limit

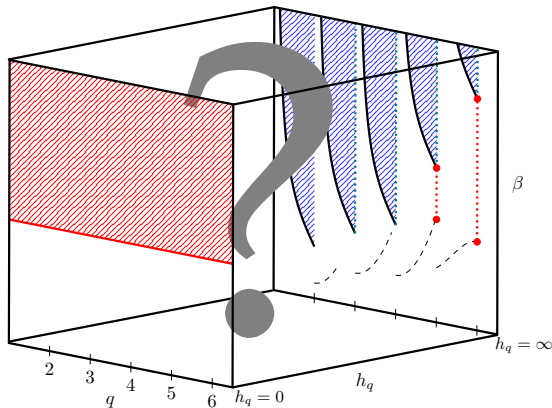


# Outline

- 1 Motivation
- 2 The Extended- $O(2)$  Model
  - The  $h_q \rightarrow \infty$  limit
  - Phase Diagram
- 3 Phase Diagram at Finite- $h_q$
- 4 Summary & Outlook

# Phase Diagram

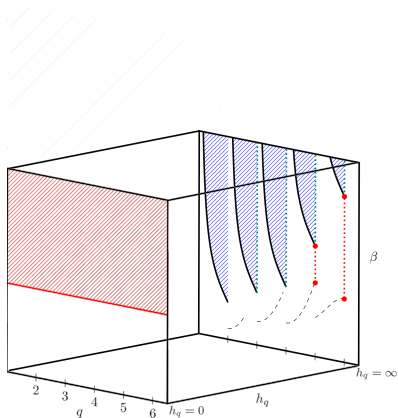
$$S = - \sum_{x,\mu} \cos(\varphi_{x+\hat{\mu}} - \varphi_x) - h_q \sum_x \cos(q\varphi_x)$$





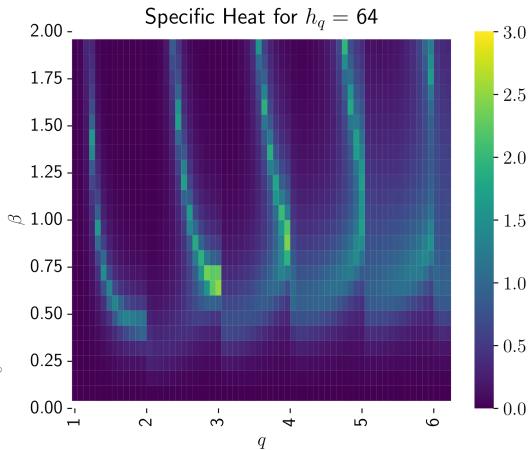
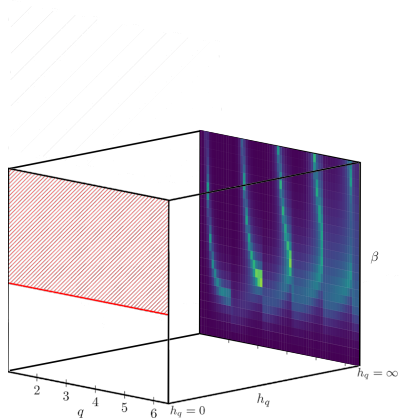
# Phase Diagram at Finite- $h_q$

$$S_{\text{ext-O}(2)} = - \sum_{x,\mu} \cos(\varphi_{x+\hat{\mu}} - \varphi_x) - h_q \sum_x \cos(q\varphi_x)$$



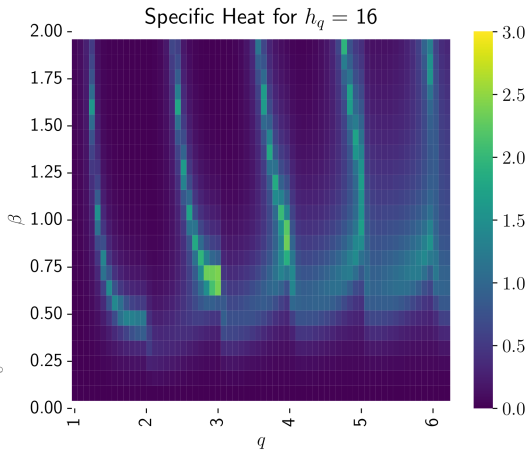
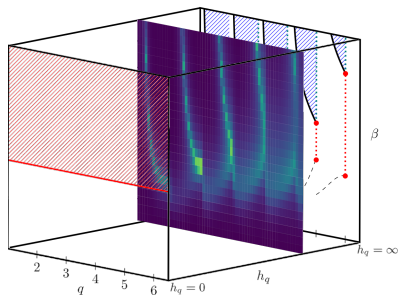
# Specific Heat from TRG with $L = 1024$ and $h_q = 64$

$$S_{\text{ext-O}(2)} = - \sum_{x,\mu} \cos(\varphi_{x+\hat{\mu}} - \varphi_x) - h_q \sum_x \cos(q\varphi_x)$$



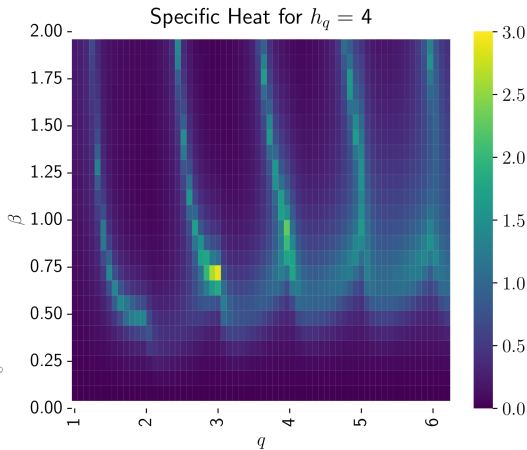
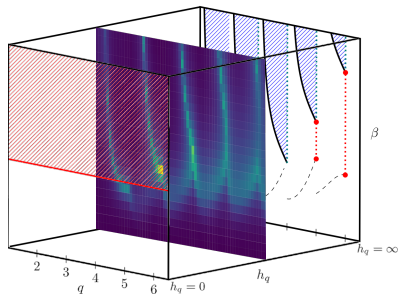
# Specific Heat from TRG with $L = 1024$ and $h_q = 16$

$$S_{\text{ext-O}(2)} = - \sum_{x,\mu} \cos(\varphi_{x+\hat{\mu}} - \varphi_x) - h_q \sum_x \cos(q\varphi_x)$$



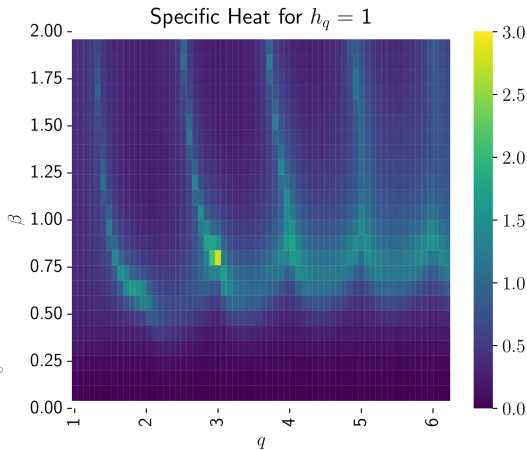
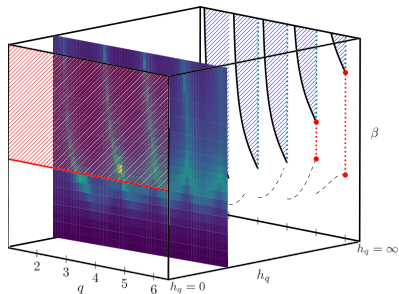
# Specific Heat from TRG with $L = 1024$ and $h_q = 4$

$$S_{\text{ext-}O(2)} = - \sum_{x,\mu} \cos(\varphi_{x+\hat{\mu}} - \varphi_x) - h_q \sum_x \cos(q\varphi_x)$$



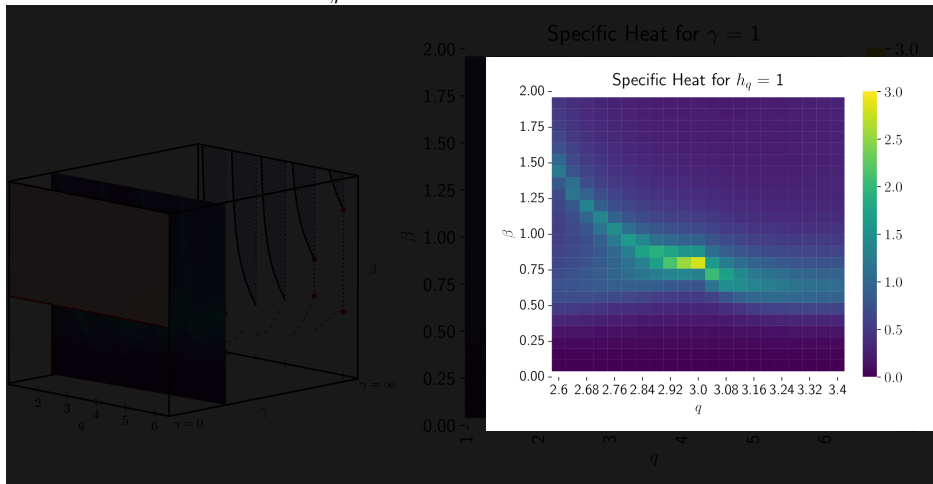
# Specific Heat from TRG with $L = 1024$ and $h_q = 1$

$$S_{\text{ext-O}(2)} = - \sum_{x,\mu} \cos(\varphi_{x+\hat{\mu}} - \varphi_x) - h_q \sum_x \cos(q\varphi_x)$$



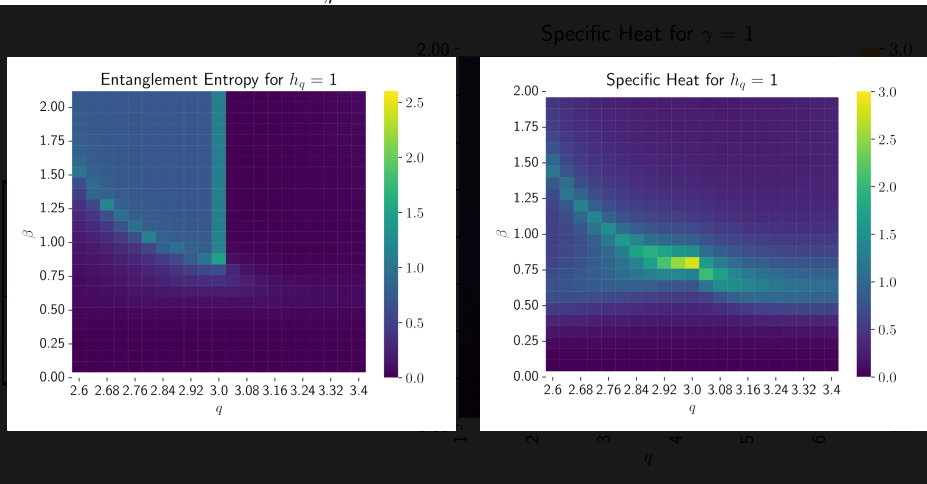
# Specific Heat from TRG with $L = 1024$ and $h_q = 1$

$$S_{\text{ext-}O(2)} = - \sum_{x,\mu} \cos(\varphi_{x+\hat{\mu}} - \varphi_x) - h_q \sum_x \cos(q\varphi_x)$$



# Specific Heat from TRG with $L = 1024$ and $h_q = 1$

$$S_{\text{ext-}O(2)} = - \sum_{x,\mu} \cos(\varphi_{x+\hat{\mu}} - \varphi_x) - h_q \sum_x \cos(q\varphi_x)$$



# Noninteger $q$ with TRG

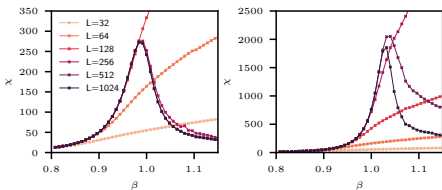


**Figure:** Magnetic susceptibility from TRG for  $q = 4.1$  near the small- $\beta$  peak for  $h_q = 0.01$  (left) and  $h_q = 0.001$  (right). For sufficiently large volumes, the magnetic susceptibility peaks plateau—implying a crossover.

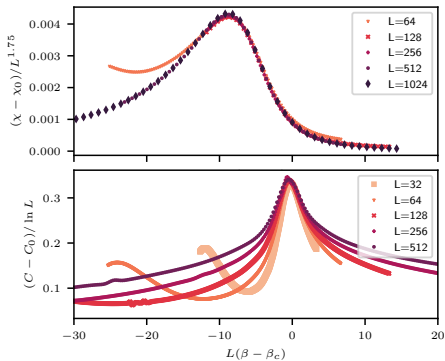


**Figure:** Data collapse of the magnetic susceptibility (top) and specific heat (bottom) from TRG near the large- $\beta$  peak for  $q = 3.9$  and  $h_q = 1$ . Consistent with Ising phase transition.



# Integer $q$ with MC

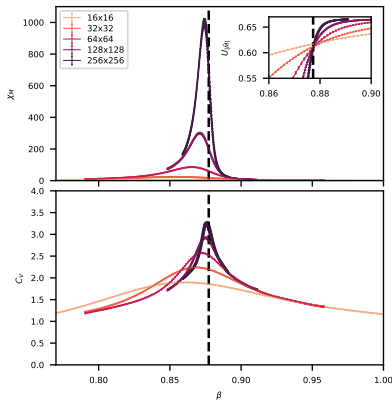


**Figure:** Magnetic susceptibility (top) and specific heat (bottom) from MC with  $q = 2$  and  $h_q = 0.1$ . Looks like an Ising phase transition.

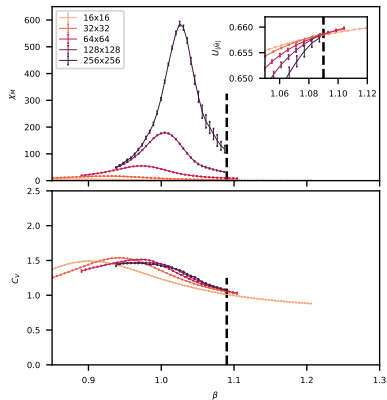


**Figure:** Magnetic susceptibility (top) and specific heat (bottom) from MC with  $q = 4$  and  $h_q = 0.1$ . Looks like a BKT phase transition.

# Integer $q$ : Finite Size Scaling

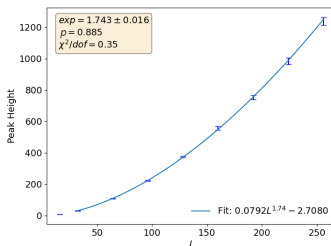
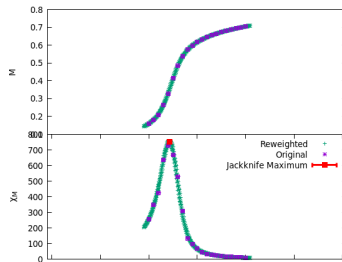
$$\left. \frac{dU_M}{d\beta} \right|_{max} = U_0 + U_1 L^{1/\nu}$$

$$C_V|_{max} = C_0 + C_1 L^{\alpha/\nu}$$

$$\langle M \rangle|_{infl} = M_0 + M_1 L^{-\beta/\nu}$$

$$\chi_M|_{max} = \chi_0 + \chi_1 L^{\gamma/\nu}$$

$$F(\vec{q})|_{max} = F_0 + F_1 L^{2-\eta}.$$



# Integer $q$ : Finite Size Scaling

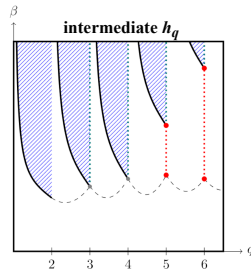
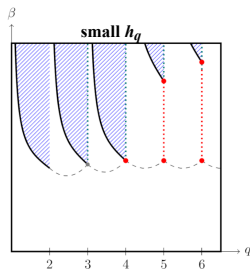
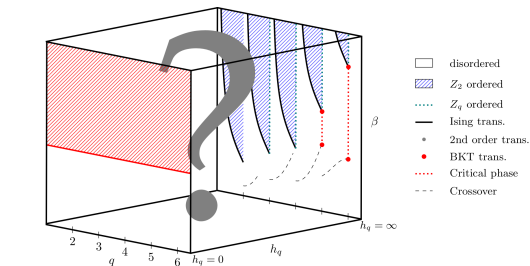
$q$	$\alpha$	$\beta$	$\gamma$	$\delta$	$\eta$	$\nu$	$\beta_c$
2	0	1/8	7/4	15	1/4	1	$\frac{1}{2} \ln(1 + \sqrt{2})$
3	1/3	1/9	13/9	14	4/15	5/6	$\frac{2}{3} \ln(1 + \sqrt{3})$
4	0	1/8	7/4	15	1/4	1	$\ln(1 + \sqrt{2})$

**Table:** The critical exponents (for reference) for the integer  $q$  clock model for  $q = 2, 3, 4$ . The clock model is the  $h_q \rightarrow \infty$  limit of the Extended- $O(2)$  model.

$q$	$h_q$	$\nu$	$\alpha$	$\beta$	$\gamma$	$\eta$
2	0.1	1.044(53)	0.021(18)	0.319(94)	1.859(96)	0.287(13)
2	1.0	1.022(71)	-0.010(16)	N/A	1.78(12)	0.251(14)
3	0.1	0.658(24)	0.354(35)	N/A	1.291(45)	0.3651(93)
3	1.0	0.809(26)	0.311(21)	N/A	1.411(36)	0.295(16)
4	0.1	2.49(89)	-0.30(12)	0.76(87)	4.3(1.5)	0.2570(85)
4	1.0	1.20(14)	-0.162(19)	0.78(61)	2.09(24)	0.2532(93)
5	0.1	N/A	N/A	N/A	N/A	0.2716(72)
5	1.0	N/A	N/A	N/A	N/A	0.2653(94)
6	0.1	N/A	N/A	N/A	N/A	0.2880(86)
6	1.0	N/A	N/A	N/A	N/A	0.2654(92)

**Table:** Critical exponents obtained via finite-size scaling.

# Phase Diagram



# Outline

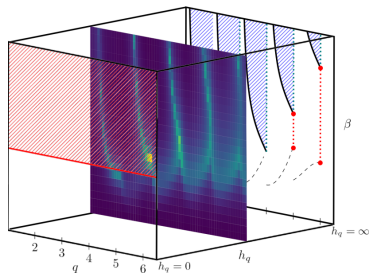
- 1 Motivation
- 2 The Extended- $O(2)$  Model
  - The  $h_q \rightarrow \infty$  limit
  - Phase Diagram
- 3 Phase Diagram at Finite- $h_q$
- 4 Summary & Outlook

# Summary & Outlook

- 1 We looked at an extended  $O(2)$  model with parameters  $\beta$ ,  $h_q$ , and  $q$

$$S = - \sum_{x,\mu} \cos(\varphi_{x+\hat{\mu}} - \varphi_x) - h_q \sum_x \cos(q\varphi_x)$$

- 2 The symmetry-breaking term allows us to explore the role of symmetry and to study the  $U(1) \rightarrow \mathbb{Z}_q$  approximations and to consider also noninteger  $q$
- 3 This model may be a good candidate for analog quantum simulation
- 4 Rich phase diagram with crossovers, second-order phase transitions of various universality classes and BKT transitions



Thank you!

Additional Slides:

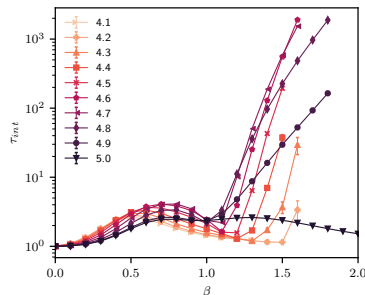


## Previous Work on the Extended- $O(2)$ Model

- José, Kadanoff, Kirkpatrick, and Nelson, Phys. Rev. B 16, 1217 (1977).
- Landau, Journal of Magnetism and Magnetic Materials 31-34, 1115 (1983)
- Hu and Ying, Physica A: Statistical Mechanics and its Applications 140, 585 (1987)
- Bramwell, Holdsworth, and Rothman, Modern Physics Letters B 11, 139 (1997)
- Calabrese and Celi, Phys. Rev. B 66, 184410 (2002)
- Rastelli, Regina, and Tassi, Phys. Rev. B 69, 174407 (2004)
- Rastelli, Regina, and Tassi, Phys. Rev. B 70, 174447 (2004)
- Taroni, Bramwell, and Holdsworth, Journal of Physics: Condensed Matter 20, 275233 (2008)
- Nguyen and Ngo, Advances in Natural Sciences: Nanoscience and Nanotechnology 8, 015013 (2017)
- Chlebicki and Jakubczyk, Phys. Rev. E 100, 052106 (2019)
- Butt, Jin, Osborn, and Saleem, (2022), arXiv:2205.03548

# TRG for Extended- $q$ -state Clock Model

- In the Monte Carlo approach, we use a Markov chain importance-sampling algorithm to generate equilibrium configurations
  - ▶ Monte Carlo has difficulty sampling this model appropriately at  $\beta > 1$  for  $q \notin \mathbb{Z}$
  - ▶ Integrated autocorrelation time explodes, and we have to perform billions of heatbath sweeps already on a  $4 \times 4$  lattice
  - ▶ Studying this model on larger lattices with Monte Carlo is challenging
- Tensor renormalization group (TRG) approach can be used instead
  - ▶ We validate TRG against Monte Carlo in the regime accessible to Monte Carlo
  - ▶ Then we use TRG to explore lattice sizes and  $\beta$ -values beyond the reach of Monte Carlo



# Algorithm Developments Needed for Extended- $O(2)$ Model

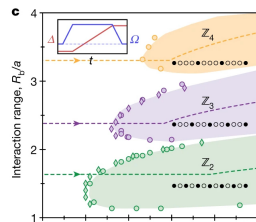
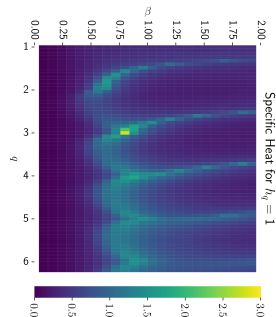
- In the  $h_q \rightarrow \infty$  limit, the DOF could be treated as discrete
  - ▶ Which means we could use an MCMC *heatbath* algorithm
  - ▶ We could use a TRG method for large volumes
- The model is more difficult to study at finite  $h_q$
- For finite  $h_q$ , the DOF are continuous
  - ▶ MCMC heatbath is not an option, so we're left with the Metropolis, which suffers from low acceptance rates and leads to large autocorrelations in this model
  - ▶ Furthermore, our TRG method was only designed for the  $h_q \rightarrow \infty$  limit
- We needed to make some algorithmic developments
  - ▶ We implemented a *biased Metropolis heatbath algorithm*<sup>18</sup> (BMHA) which is designed to approach heatbath acceptance rates
  - ▶ To explore large volumes, Ryo Sakai implemented a Gaussian quadrature method

---

<sup>18</sup>A. Bazavov and B. A. Berg, PRD 71, 114506 (2005)

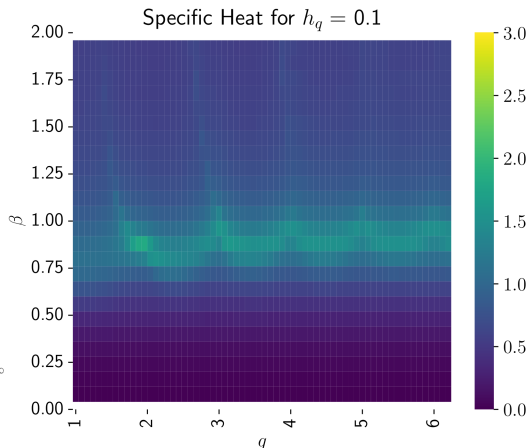
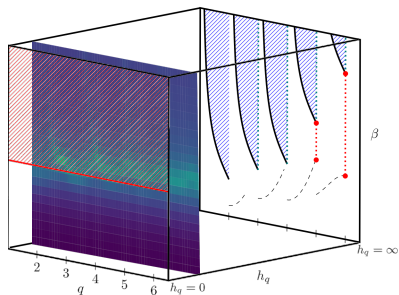
# Connections to Quantum Simulation

- ❶ Field digitization in quantum simulation
  - ❶ Can approximate  $U(1)$  by  $\mathbb{Z}_q$
  - ❷ Need to optimize the approximation
  - ❸ It is useful to have a continuous family of models that interpolate among the different  $q$
- ❷ The extended- $O(2)$  model shows interesting behavior already on very small lattices making it a good test case for analog simulation
- ❸ Quantum simulation of similar models with a continuously tunable parameter have been done with Rydberg atoms (Bernien et. al. Nature 551, 579-584 (2017), Keesling et. al. Nature 568, 207 (2019))
  - The resulting phase diagram (right) shows similarities to the phase diagram of the extended- $O(2)$  model at finite  $h_q$ .

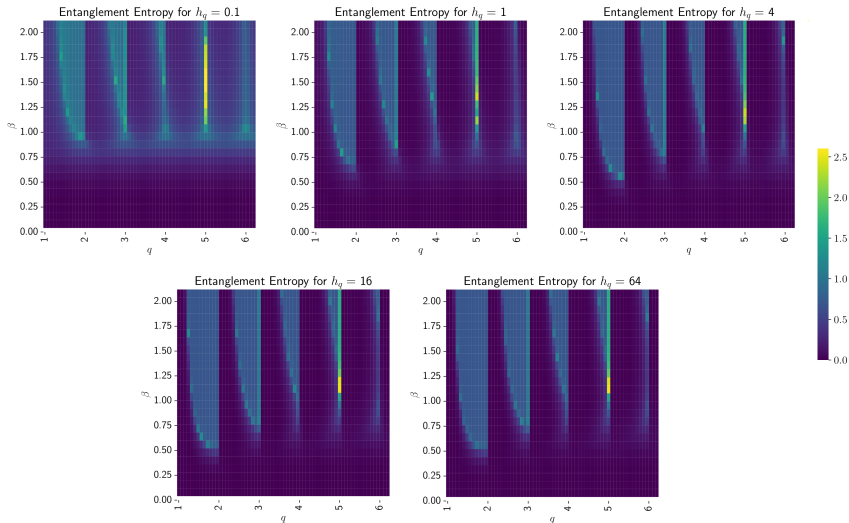


# Specific Heat from TRG with $L = 1024$ and $h_q = 0.1$

$$S_{\text{ext-O}(2)} = - \sum_{x, \mu} \cos(\varphi_{x+\hat{\mu}} - \varphi_x) - h_q \sum_x \cos(q\varphi_x)$$

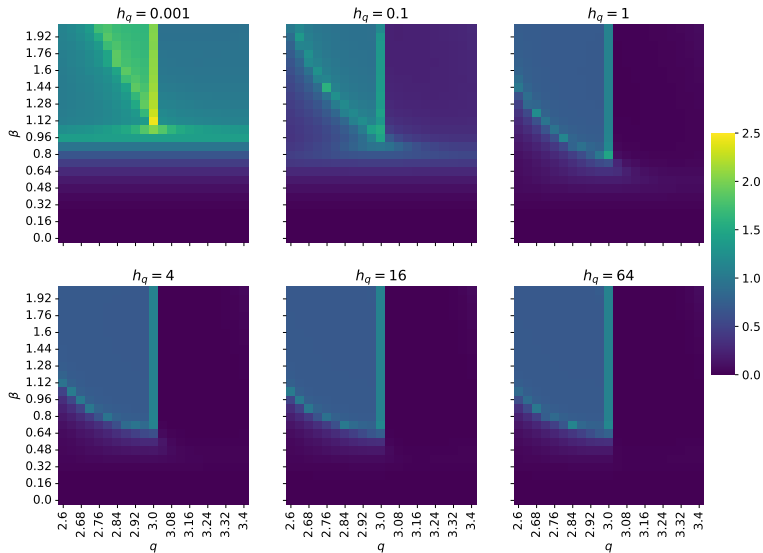


# Entanglement Entropy from TRG with $L = 1024$



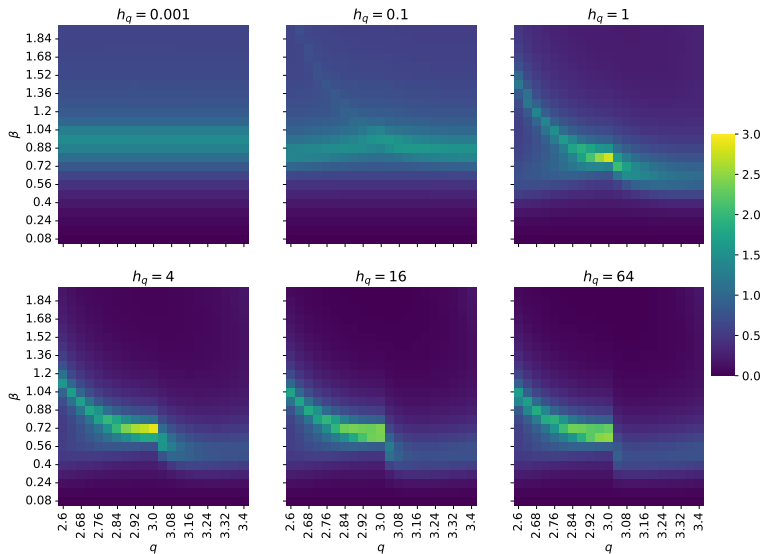
# Entanglement Entropy from TRG with $L = 1024$

Entanglement Entropy near  $q = 3$



# Specific Heat from TRG with $L = 1024$

Specific Heat near  $q = 3$





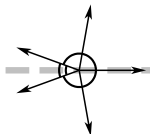
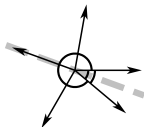
# Choice of $\varphi_0$

- Choice of  $\varphi_0$  can change the DOF in the model
- We choose  $\varphi_0 = 0$ , i.e.  $\varphi \in [0, 2\pi)$ , but we also investigate  $\varphi_0 = -\pi$

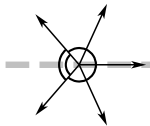
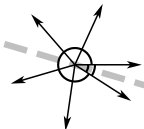
$$\varphi_0 = 0$$

$$\varphi_0 = -\pi$$

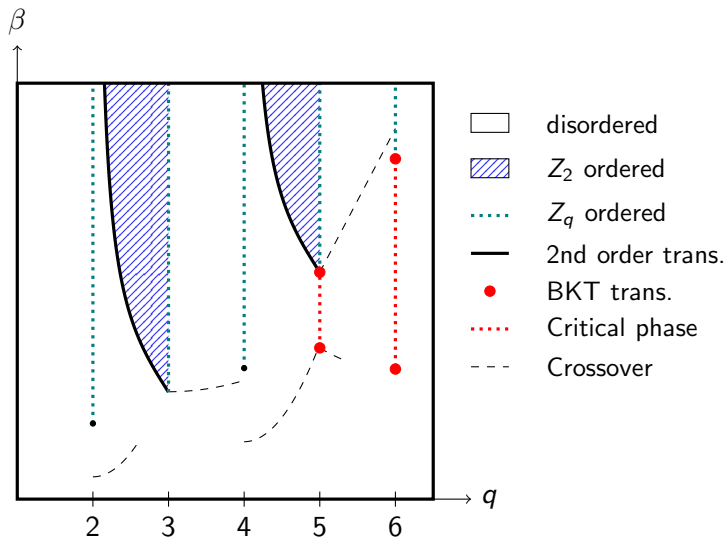
$$q = 4.5$$



$$q = 5.5$$



# Phase diagram for $h_q = \infty$ and $\varphi_0 = -\pi$



# Placement of $\beta$

- One can define the model as

$$S = -\beta \sum_{x,\mu} \cos(\varphi_{x+\hat{\mu}} - \varphi_x) - h_q \sum_x \cos(q\varphi_x)$$

where  $\beta$  is multiplying the first term like a field-theoretic coupling. Then the Boltzmann factor is  $e^{-S}$

- Alternatively, one can factor  $\beta$  out front and define the model as

$$S = - \sum_{x,\mu} \cos(\varphi_{x+\hat{\mu}} - \varphi_x) - h'_q \sum_x \cos(q\varphi_x)$$

with Boltzmann factor  $e^{-\beta S}$ , where  $\beta$  is the inverse temperature

- The two definitions are related by  $h'_q = h_q/\beta$
- We have used both definitions, however, the Monte Carlo results shown in these slides are from the definition with  $\beta$  factored out front

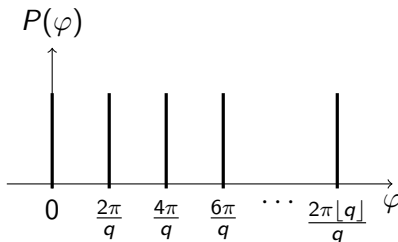
# The Need to Shift the Angles: A Subtlety

- In the ordinary clock model, we have the energy function

$$S = - \sum_{\langle x,y \rangle} \cos(\varphi_x - \varphi_y)$$

- The angles  $\varphi_x^{(k)}$  are selected discretely as  $\varphi_0 \leq \varphi_x^{(k)} = \frac{2\pi k}{q} < \varphi_0 + 2\pi$
- When  $\beta = 0$  and with  $\varphi_0 = 0$ , the spins are selected uniformly from a “Dirac comb”

$$P_{q,\varphi_0=0}^{clock}(\varphi) \sim \sum_{k=0}^{\lfloor q \rfloor} \delta\left(\varphi - \frac{2\pi k}{q}\right)$$



# The Need to Shift the Angles: A Subtlety

- In the Extended-O(2) model, we have the energy function

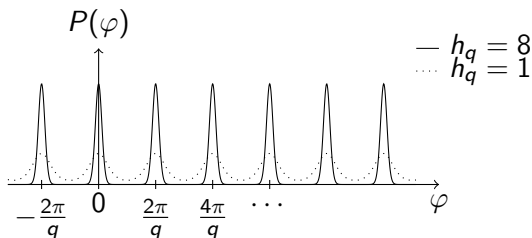
$$S = - \sum_{\langle x,y \rangle} \cos(\varphi_x - \varphi_y) - h_q \sum_x \cos(q\varphi_x)$$

- The angles  $\varphi_x$  are now selected continuously in

$$\varphi_0 \leq \varphi \in \mathbb{R} < \varphi_0 + 2\pi$$

- When  $\beta = 0$  and with  $\varphi_0 = 0$ , the spins are selected from a distribution

$$P_{q,\varphi_0}^{\text{extO2}}(\varphi) \sim e^{h_q \cos(q\varphi)}$$



# The Need to Shift the Angles: A Subtlety

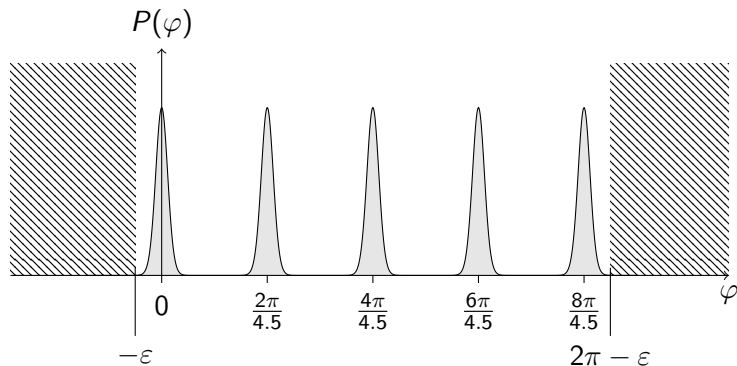


Figure: To recover the Dirac comb of the clock model distribution in the  $h_q \rightarrow \infty$  limit, the angle domain must be shifted by some  $\varepsilon$  so that the histogram includes all relevant peaks.

# The Need to Shift the Angles: A Subtlety

- To match the clock model in the  $h_q \rightarrow \infty$  limit, it should be sufficient to choose  $\varepsilon$  such that

$$P_{q,\varphi_0}^{\text{extO2}}(\varphi) \xrightarrow{h_q \rightarrow \infty} P_{q,\varphi_0}^{\text{clock}}(\varphi)$$

where for the clock model, angles are selected from  $[\varphi_0, \varphi_0 + 2\pi)$ , but for the Extended-O(2) model, they are selected from  $[\varphi_0 - \varepsilon, \varphi_0 - \varepsilon + 2\pi)$

- In our case, we use  $\varphi_0 = 0$ , and choose

$$\varepsilon = \pi \left( 1 - \frac{\lfloor q \rfloor}{q} \right)$$

so that the  $\lfloor q \rfloor$  peaks of the distribution  $P_{q,\varphi_0}^{\text{extO2}}(\varphi)$  are centered in the domain  $[-\varepsilon, 2\pi - \varepsilon)$